Development 138, 317-326 (2011) doi:10.1242/dev.057299

Hindbrain patterning requires fine-tuning of early *krox20* transcription by Sprouty 4

Charlotte Labalette[1,2,3], Yassine Xavier Bouchoucha[1,2,3], Michel Adam Wassef[1,2,3], Patricia Anne Gongal[1,2,3], Johan Le Men[1,2,3], Thomas Becker[4], Pascale Gilardi-Hebenstreit[1,2,3] and Patrick Charnay[1,2,3,*]

SUMMARY

Vertebrate hindbrain segmentation is an evolutionarily conserved process that involves a complex interplay of transcription factors and signalling pathways. Fibroblast growth factor (FGF) signalling plays a major role, notably by controlling the expression of the transcription factor Krox20 (Egr2), which is required for the formation and specification of two segmental units: rhombomeres (r) 3 and 5. Here, we explore the molecular mechanisms downstream of FGF signalling and the function of Sprouty 4 (Spry4), a negative-feedback regulator of this pathway, in zebrafish. We show that precise modulation of FGF signalling by Spry4 is required to determine the appropriate onset of *krox20* transcription in r3 and r5 and, ultimately, rhombomere size in the r3-r5 region. FGF signalling acts by modulating the activity of *krox20* initiator enhancer elements B and C; in r5, we show that this regulation is mediated by direct binding of the transcription factor MafB to element B. By contrast, FGF signalling does not control the *krox20* autoregulatory element A, which is responsible for amplification and maintenance of *krox20* expression. Therefore, early *krox20* transcription sets the blueprint for r3-r5 patterning. This work illustrates the necessity for fine-tuning in a common and fundamental patterning process, based on a bistable cell-fate choice involving the coupling of an extracellular gradient with a positive-feedback loop. In this mode of patterning, precision and robustness can be achieved by the introduction of a negative-feedback loop, which, in the hindbrain, is mediated by Spry4.

KEY WORDS: FGF, Segmentation, Rhombomere, Feedback loop, Zebrafish

INTRODUCTION

Vertebrate hindbrain morphogenesis has been the focus of intensive study as a model for vertebrate patterning. The establishment of hindbrain anteroposterior (AP) identity involves a transient segmentation, which leads to the formation of seven to eight metameres called rhombomeres (r) (Lumsden, 1990; Lumsden and Krumlauf, 1996). These territories constitute compartments and developmental units for neuronal differentiation, branchiomotor nerve organisation and neural crest specification (Lumsden and Keynes, 1989). The gene regulatory network underlying hindbrain segmentation includes several transcription factor genes that show spatially restricted patterns of expression along the AP axis, with limits corresponding to prospective or established boundaries between adjacent rhombomeres (Lumsden and Krumlauf, 1996). Among them, *Krox20* (also known as *Egr2*) is specifically expressed in r3 and r5 (Wilkinson et al., 1989) and has been shown to be essential for the establishment and specification of these rhombomeres (Schneider-Maunoury et al., 1993; Schneider-Maunoury et al., 1997; Swiatek and Gridley, 1993; Voiculescu et al., 2001). However, how relative rhombomere sizes are controlled, an essential issue related to many patterning and morphogenetic processes, has not been addressed.

Control of hindbrain segmentation involves several cell signalling pathways. Among them, Fibroblast growth factor (FGF) signalling is necessary in particular to promote Krox20-mediated r3 and r5 development (Aragon and Pujades, 2009; Marin and Charnay, 2000; Maves et al., 2002; Walshe et al., 2002; Wiellette and Sive, 2003; Wiellette and Sive, 2004). It has been shown in zebrafish and chick embryos that *Krox20* expression requires prior FGF signalling (Aragon and Pujades, 2009; Walshe et al., 2002). However, the molecular mechanisms of this regulation have not been investigated. Furthermore, despite the importance of FGF signalling in hindbrain patterning, its possible modulation by antagonists has not been analysed. A negative regulator of the FGF pathway, Sprouty (Spry; Sty – FlyBase), has been identified in *Drosophila* (Hacohen et al., 1998). *spry* is induced by FGF signalling and therefore functions as a negative-feedback regulator (Hacohen et al., 1998). Spry acts intracellularly, through inhibition of the Ras/MAPK pathway (Gross et al., 2001; Yusoff et al., 2002). Four vertebrate orthologues of *spry* have been identified. In mice, *Spry1*, *Spry2* and *Spry4* are widely expressed in the embryo, whereas *Spry3* expression is restricted to the adult (Minowada et al., 1999).

In this study, we have investigated the role of Spry genes in zebrafish hindbrain development and show that Spry4 plays a key role in hindbrain patterning, controlling the relative size of odd- and even-numbered rhombomeres in the r3-r5 region. We demonstrate that Spry4 sets the appropriate onset of *krox20* transcription in r3 and r5 by fine-tuning FGF control of *krox20* initiator enhancer elements. By contrast, Spry4 and FGF signalling do not affect the activity of the *krox20* autoregulatory element responsible for the later amplification and maintenance of *krox20* expression. Therefore, the size of mature rhombomeres is determined at the onset of *krox20* expression, and this work

[1]Ecole Normale Supérieure, IBENS, Paris Cedex 75230, France. [2]Inserm, U1024, Paris Cedex 75230, France. [3]CNRS, UMR 8197, Paris Cedex 75230, France. [4]Brain and Mind Research Institute, Sydney Medical School, 100 Malett St, Camperdown NSW 2050, Australia.

*Author for correspondence (charnay@biologie.ens.fr)

Accepted 15 November 2010

presents a mechanism that combines negative and positive autoregulatory loops to achieve precise and robust pattern formation.

MATERIALS AND METHODS

In situ hybridisation

To generate a *spry1* probe, a cDNA was subcloned into the pCRII-TOPO vector, after RT-PCR using primers 5′-GAATTCGTCCTGTCCCTG-GACCAG-3′ and 5′-CTCGAGCTTTAACGCAGCCTTTCG-3′. For the *spry2* and *spry4* probes, the 3′UTR regions (IMAGE 7227962 and IMAGE 3719315, respectively) were subcloned into pBluescript (Stratagene). Other probes used were zebrafish *krox20* (Oxtoby and Jowett, 1993), chicken *Krox20* (Giudicelli et al., 2001), *ntl* (Schulte-Merker et al., 1994), *her5* (Muller et al., 1996), *mafba* (Moens et al., 1998), *fgf8* (Furthauer et al., 1997) and *hoxb1a* (Prince et al., 1998). Single and double whole-mount in situ hybridisations were performed as described (Hauptmann and Gerster, 1994).

Constructs and zebrafish lines

For all constructs, cloning junction and point mutations were verified by sequencing. The pCS2-spry4 vector was obtained by subcloning the zebrafish *spry4* open reading frame into pCS2+ (RZPD). To generate the dominant-negative form of Spry4 (Spry4Y52A), a mutation of TAC (tyrosine) to GCC (alanine) was introduced at codon 52 (Sasaki et al., 2001) using the Transformer Site-Directed Mutagenesis Kit (Clontech). A morpholino-resistant *spry4* RNA was generated by introducing five silent mismatches into the morpholino target sequence: 5′-(C>G)AGATG-GA(G>A)TC(A>T)(A>T)GGGT(T>G)-3′. For electroporation in the chick neural tube, wild-type and dominant-negative *spry4* cDNAs were tagged with a sequence encoding an HA epitope (5′-TACCCATACGACG-TACCAGACTACGCATCG-3′) just before the stop codon and subcloned into the pAdRSV vector (Wassef et al., 2008). Chicken elements A and B were cloned upstream of the *gfp* reporter in a modified pTol2 vector (Stedman et al., 2009). Chicken element C was cloned into pBGZ40 (Yee and Rigby, 1993) upstream of the minimal β-*globin* promoter-*gfp* reporter. The mutations in the MafB binding sites were introduced using the Phusion Site-Directed Mutagenesis Kit (Finnzymes) and/or the QuikChange Multi Site-Directed Mutagenesis Kit (Stratagene). To generate the *zB:gfp* construct, a 720 bp zebrafish element B (PCR amplified using primers 5′-GATATGCATGGTAAAATCTCCCACCATCG-3′ and 5′-GCGCTC-GAGCACCGCCGAAAAACAATAGC-3′) was cloned upstream of the *gfp* reporter in the modified pTol2 vector. Transgenic lines were obtained from embryos injected at the 1-cell stage with the pTol2 constructs together with *tol2 transposase* mRNA.

mRNA and morpholino injections

spry4 capped sense RNAs were obtained using the mMESSAGE mMACHINE Kit (Ambion) and 300 pg were injected at the 1-cell stage. The sequence of the *spry1* morpholino (Spry1mo) is 5′-CGCG-GAGATCCATAAGACACGATCA-3′. Morpholinos for *spry2* and *spry4* (Spry2mo and Spry4mo) have been described previously (Furthauer et al., 2001; Furthauer et al., 2004). A control *spry4* morpholino (Ctrlmo) was designed by introducing five mismatches into Spry4mo (5′-GTAA-CACTTGAATCGATCTGAAGGT-3′). Morpholinos (Gene Tools) were diluted in Danieau buffer and 2 pmoles were injected at the 1- to 4-cell stage.

Proliferation assay, phosphorylation analysis and SU5402 treatment

For proliferation assays, embryos were immunostained using a rabbit polyclonal antibody against phospho-Histone H3 (Upstate) and Alexa 488-coupled goat anti-rabbit IgG (Jackson). This analysis was preceded by fluorescent in situ hybridisation for *krox20* using FastRed substrate (Roche). Confocal optical sections of flat-mounted embryos were obtained with an inverted Leica DMIRE2 microscope. Western blot analysis was performed as described (Pezeron et al., 2008) using monoclonal phosphoERK (Cell Signaling), polyclonal ERK (Cell Signaling) and monoclonal β-actin (Sigma) antibodies. The phosphoERK and total ERK levels on the immunoblots were quantified using ImageJ software (NIH). Polyclonal phosphoERK antibody (Cell Signaling) was used for whole-mount immunostaining. Treatment of embryos with 60 μM SU5402 was performed as described (Walshe et al., 2002).

In ovo electroporation, X-gal staining and whole-mount immunostaining

In ovo electroporation of the chick neural tube, recovery of embryos and immunodetection were performed as previously described (Desmazières et al., 2009). GFP expression was detected using a rabbit polyclonal antibody (Molecular Probes). Fluorescent signals were quantified using ImageJ. X-gal staining was performed as described (Ghislain et al., 2003).

Gel retardation analysis

Band shift assays were performed with MafB protein purified from bacterial extracts as described (Manzanares et al., 2002). The following double-stranded oligonucleotides were used as probes or competitors: wtM1, 5′-GGAAAGTACAGACAGTGCATTTTCCC-3′; mutM1, 5′-GGAAAGGTAAGACAGTGCATTTTCCC-3′; wtM2, 5′-CAAATTTG-CTGATTTTCACCAGTATC-3′; and mutM2, 5′-CAAATTGCAT-GATTTTCACCAGTATC-3′.

RESULTS

Expression of the Sprouty gene family in the developing hindbrain

In the zebrafish embryo, expression of *spry1*, *spry2* and *spry4* has been reported in the midbrain-hindbrain region at mid-somitogenesis stages (Furthauer et al., 2001; Furthauer et al., 2002; Furthauer et al., 2004; Komisarczuk et al., 2008). To further analyse their expression, we performed an in situ hybridisation analysis starting from 80% epiboly. We found that these genes were expressed from 90% epiboly in a large transverse stripe of the neural plate, which is likely to correspond to the prospective hindbrain (data not shown). At 100% epiboly, *spry1* was still expressed in a broad band corresponding approximately to the hindbrain (Fig. 1A), whereas *spry2* and *spry4* showed more restricted AP patterns within the hindbrain (Fig. 1B,C). At the 1-somite stage, to evaluate the limits of the Spry gene expression domains, we performed double in situ hybridisations with *krox20*. At this stage, *krox20* expression is well established in r3, but is only beginning to be initiated in prospective r5. *spry1* was expressed from approximately r1 to r6 (Fig. 1D) and *spry2* from r1/r2 to r4 (Fig. 1E). In contrast to *spry1* and *spry2*, which were uniformly expressed in single domains, *spry4* showed strong expression in r2 and r3 and weaker expression in r4 and r5 (Fig. 1F). At the 4- to 6-somite stages, *spry1* and *spry2* were highly expressed in r1, ventral r2 and r4, and in the midbrain-hindbrain boundary (MHB) (Fig. 1G,H,J,K). By contrast, *spry4* expression became prominent in r3, r5 and the MHB (Fig. 1I,L).

Spry4 controls hindbrain patterning in the r3-r5 region

To investigate the effects of Spry loss-of-function on hindbrain patterning, we performed knockdown experiments with morpholino oligonucleotides. We used morpholinos that had been previously tested: Spry1mo (Marika Kapsimali, personal communication), Spry2mo (Furthauer et al., 2004) and Spry4mo (Furthauer et al., 2001). As a control we used a version of Spry4mo containing five mismatches (Ctrlmo). To evaluate the consequences of morpholino injections, we first performed double in situ hybridisations at the 10-somite stage for *krox20* and *her5*, a marker of the MHB. Spry1mo-injected embryos (n=23) did not show any obvious phenotype (Fig. 2A,B). Spry2mo induced a lateral broadening of the neural plate and a shortening of the AP axis

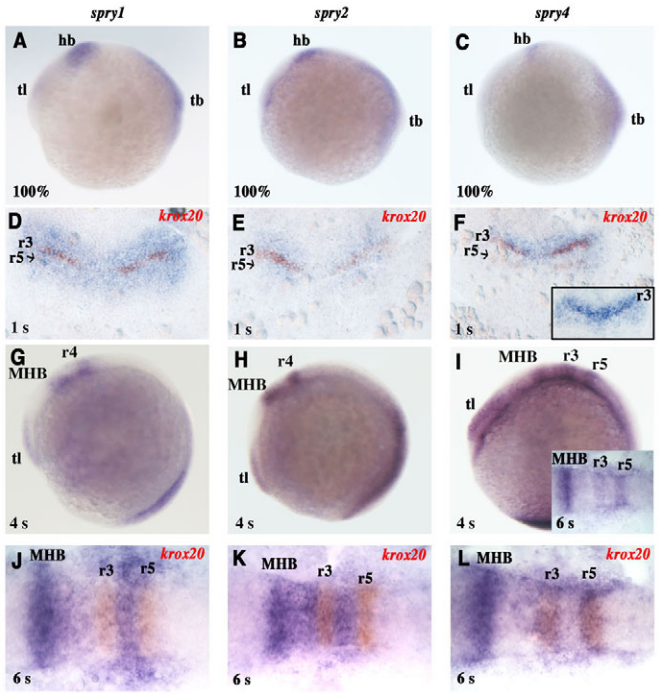

Fig. 1. Spry gene expression in the early zebrafish hindbrain. (**A-L**) In situ hybridisations were performed with *spry1* (A,D,G,J), *spry2* (B,E,H,K) and *spry4* (C,F,I,L) probes (blue) at the indicated somite (s) or epiboly (%) stages, shown as lateral views with anterior to the left (A-C,G-I) and flat-mounts with anterior at the top (D-F) or left (inset in I and J-L). Where indicated (D-F,J-L), double in situ hybridisation was performed with a *krox20* probe (red) to allow precise localisation of r3 and r5. The inset in F shows the *spry4* pattern without *krox20* labelling. hb, hindbrain; tb, tailbud; tl, telencephalon; MHB, midbrain-hindbrain boundary.

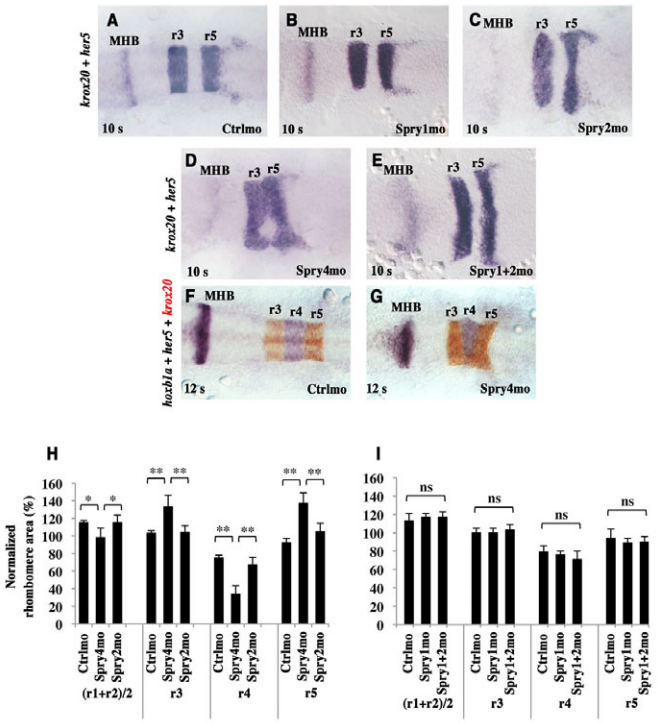

Fig. 2. Spry4 loss-of-function results in hindbrain patterning defects. (**A-G**) Zebrafish embryos injected with either control morpholino (Ctrlmo) (A,F), Spry1mo (B), Spry2mo (C), Spry4mo (D,G) or both Spry1mo and Spry2mo (E) were collected at the 10-somite (A-E) or 12-somite (F,G) stage and subjected to in situ hybridisation for *krox20* and *her5*, a marker of the MHB (A-E, both purple), or for *krox20* (red), *her5* and *hoxb1a* (purple) (F,G). Embryos are flat-mounted with anterior to the left. (**H**,**I**) Quantitative evaluation of rhombomere areas. Normalised areas were obtained by dividing each rhombomere area by one fifth of the area of the neural plate from r1 to r5. ns, not significant ($P>0.05$); *, $P<0.004$; **, $P<0.0001$; Student's *t*-test. Errors bars indicate s.e.m.

(n=22; Fig. 2C). These malformations might result from dorsalisation and/or convergent-extension defects, as previously described (Furthauer et al., 2004). As expected (Furthauer et al., 2001), similar malformations were observed in Spry4mo-injected embryos (Fig. 2D). The severity of these morphological defects was comparable between Spry2 and Spry4 morphants (for quantification, see Fig. S1 in the supplementary material). However, Spry4mo injection resulted in an additional phenotype, with a dramatic reduction of the area of r4, often resulting in a partial fusion of r3 and r5 territories (Fig. 2D). Co-injection of the Spry4mo with a p53 morpholino (Robu et al., 2007) resulted in the same change in hindbrain patterning, excluding an artefact of morpholino-induced cell death (see Fig. S2 in the supplementary material). These modifications did not lead to any overlap between r3/r5 and r4 markers as revealed by double in situ hybridisation with *krox20* and *hoxb1a* probes (Fig. 2F,G).

Quantification of the areas of individual rhombomeres, after normalisation to the area of the r1-r5 territory, revealed a 55% decrease in the area of r4 in Spry4mo-injected embryos (n=18) as compared with controls (n=12; t-test, $P<0.0001$; Fig. 2H). By contrast, the r1/r2 territory was only decreased by 15% in Spry4 morphants (t-test, $P<0.004$) (Fig. 2H). The specific reduction in the r4 area in Spry4 morphants coincided with increases in the areas of r3 and r5 (by 29% and 48%, respectively; t-test, $P<0.0001$; Fig. 2H), suggesting that these rhombomeres had expanded at the expense of r4. No such differences in r3, r4 and r5 areas were observed in Spry1 or Spry2 morphants (Fig. 2H,I). As the Spry1 and Spry2 amino acid sequences are more closely related to each other than to that of Spry4, these proteins might have redundant functions. We therefore evaluated the consequences of combined Spry1 and Spry2 loss-of-function. Although co-injected embryos appeared highly laterally broadened, no significant change in the relative area of the rhombomeres was observed (n=25; Fig. 2E,I). Altogether, these data demonstrate that Spry4 loss-of-function specifically results in an expansion of r3 and r5, presumably at the expense of r4, and that it is unlikely that these effects are related to the morphological broadening phenotype.

We then investigated whether this mispatterning of the hindbrain persisted at later stages. At the 20-somite stage, rhombomere boundaries are well established and the formation of the neural rod is complete. In Spry4mo-injected embryos (n=18), the r4 area was reduced by 53%, as compared with control embryos (n=12; t-test, $P<0.0001$; see Fig. S3 in the supplementary material). Conversely, r3 and r5 areas were increased by 28% and 37%, respectively, as

compared with controls (*t*-test, $P<0.0001$; see Fig. S3 in the supplementary material). The specificity of the phenotype was confirmed by RNA rescue experiments. For this purpose, Spry4mo was co-injected with a full-length *spry4* mRNA that contained silent mutations in the morpholino target sequence. In Spry4 morphants co-injected with this mRNA (n=18), the reduction of the r4 area (by 11%) and the extensions of r3 and r5 (by 10% and 11%, respectively) were much milder than without co-injection (see Fig. S3 in the supplementary material), indicating that the phenotype associated with the Spry4mo was largely rescued by *spry4* mRNA and is therefore specific. Altogether, these data establish that Spry4 loss-of-function results in a permanent expansion of the r3 and r5 territories and in a commensurate reduction of r4.

Spry4 does not regulate cell proliferation

The differential expansion of r3/r5 and r4 in embryos associated with Spry4 loss-of-function might have resulted from abnormalities in the rates of cell proliferation. We investigated whether Spry4 loss-of-function differentially affected cell proliferation during early somitogenesis. We identified cells in mitosis by immunostaining with an antibody directed against phospho-Histone H3 in control (n=17) and Spry4mo-injected (n=23) embryos at the 5-somite stage. The immunostaining was combined with *krox20* mRNA detection by fluorescent in situ hybridisation to localise r3 and r5. No significant changes in the distribution of mitotic cells were observed in r3, r4 or r5 upon Spry4 knockdown (see Fig. S4 in the supplementary material). Thus, the relative expansion of r3 and r5 with respect to r4 cannot be explained by differential cell proliferation.

Spry4 modulates the onset of *krox20* expression

The expansion of r3 and r5 and the corresponding reduction of r4 in Spry4 morphants might occur during the growth of the rhombomeres or result from very early cell-fate decisions. To address this, we investigated whether Spry4 loss-of-function affected the early expression of *krox20*. To precisely stage embryos, we performed double in situ hybridisations for *krox20* and *no tail* (*ntl*). *ntl* is expressed in the germ ring and can be used to precisely evaluate the extent of tailbud closure (Fig. 3A-C, insets). In control embryos at the 100% epiboly stage, expression of *krox20* was observed in 46% of the embryos in r3, but never at the level of prospective r5 (n=24; Fig. 3A,D). By contrast, all Spry4mo-injected embryos expressed *krox20* in r3 and in a larger territory than in the controls (n=27; Fig. 3B,D). Furthermore, 22% of Spry4 morphants also expressed *krox20* in r5. This phenotype was specific to Spry4 as it did not occur in Spry2mo-injected embryos (20% expressed *krox20* in r3 and none expressed *krox20* at the level of r5; n=20; Fig. 3C,D). Similarly, Spry1 or double Spry1;Spry2 morphants did not show any detectable change in *krox20* expression compared with controls (data not shown). The specificity of this phenotype in Spry4 morphants was confirmed by rescue experiments. As shown in Fig. 3E, the phenotype was strongly reduced by co-injection of *spry4* mRNA. Thus, Spry4 loss-of-function leads to both premature *krox20* expression and larger early expression domains.

To further investigate the timing of this premature *krox20* expression, we examined earlier stages. At the 95% epiboly stage, all Spry4 morphants expressed *krox20* in r3 and 4% already showed expression at the level of prospective r5 (n=28; Fig. 3D). By contrast, *krox20* expression was detected at the level of r3 in only 27% of control and 10% of Spry2mo-injected embryos (n=26 and n=42, respectively; Fig. 3D). At the 90% epiboly stage, neither control (n=28) nor Spry2mo-injected (n=40) embryos displayed *krox20* expression (Fig. 3D). By contrast, 40% of the Spry4mo-injected embryos already expressed *krox20* at the level of prospective r3 (n=40; Fig. 3D).

To confirm these data, *krox20* expression was investigated following injection of an mRNA encoding a dominant-negative form of Spry4 (Spry4Y52A) (Sasaki et al., 2001), which is another approach to obtain loss-of-function. At the 95% epiboly stage, 70% of *spry4Y52A* mRNA-injected embryos showed *krox20* expression in r3 (n=36), in contrast to only 20% of *gfp* mRNA-injected control embryos (n=50; Fig. 3F). Therefore, consistent with the morpholino experiments, injection of the dominant-negative RNA results in premature and expanded *krox20* expression in r3.

Finally, we investigated whether we could obtain phenotypes converse to those of the loss-of-function experiments by Spry4 gain-of-function. For this purpose, we injected embryos with *spry4* mRNA. As shown in Fig. 3E, at 100% epiboly only 13% of the *spry4* mRNA-injected embryos (n=23) showed expression of *krox20* in r3, as compared with 43% of the *gfp* mRNA-injected controls (n=21; χ^2-test, $P<0.05$). *krox20* expression in r5 was also affected by the misexpression of *spry4*. At 10.25 hours post-fertilisation (hpf) 73% of the *gfp* mRNA-injected embryos expressed *krox20* in r5 (n=26) as compared with only 37% of the *spry4* mRNA-injected embryos (n=27; χ^2-test, $P<0.05$; Fig. 3G). These data indicate that *spry4* overexpression delays the onset of *krox20* expression, an effect opposite to that of Spry4 loss-of-function.

In conclusion, our results indicate that Spry4 modulates the onset and early expansion of *krox20* expression. This early phenotype correlates with the expansion of r3 and r5 territories at later stages, suggesting that early *krox20* expression is a critical determinant of the patterning of the r3-r5 region.

The onset of *krox20* expression is determined by FGF signalling

Our data indirectly implicated FGF signalling in the onset of *krox20* expression. To confirm that modulations of Spry4 activity resulted in modifications at the level of FGF signalling, we analysed activation of the ERK pathway, which is known to require FGF signalling (Aragon and Pujades, 2009; Roy and Sagerstrom, 2004). Control and Spry4mo-injected embryos were collected at 100% epiboly and western blot analysis was performed on whole embryo protein extracts, using an antibody against phosphorylated (p) ERK1/2 (Mapk3/1 – Zebrafish Information Network), a read-out of ERK pathway activation. The pERK1/2 level, normalised to total ERK1/2, was increased in Spry4 morphants (see Fig. S5 in the supplementary material). To reveal FGF signalling in situ, we performed whole-mount immunostaining against pERK1/2 and in situ hybridisation for a target of the pathway, *pea3*. pERK1/2 and *pea3* were detected in the hindbrain, and, in Spry4 morphants, their expression levels were higher (see Fig. S5 in the supplementary material). Together, these data indicate that Spry4 loss-of-function leads to enhanced FGF signalling, consistent with Spry4 acting as an antagonist of this pathway.

Previous studies have revealed that *krox20* expression at mid- and late somitogenesis stages is dependent on prior FGF signalling (Marin and Charnay, 2000; Maves et al., 2002; Walshe et al., 2002; Wiellette and Sive, 2003). However, the role of the pathway has not been examined at early stages of *krox20* expression. To directly investigate this, we treated embryos with SU5402, an inhibitor of FGF receptor activity, from 50% epiboly. We first checked that this treatment prevented expression of *spry4* at the 100% epiboly stage

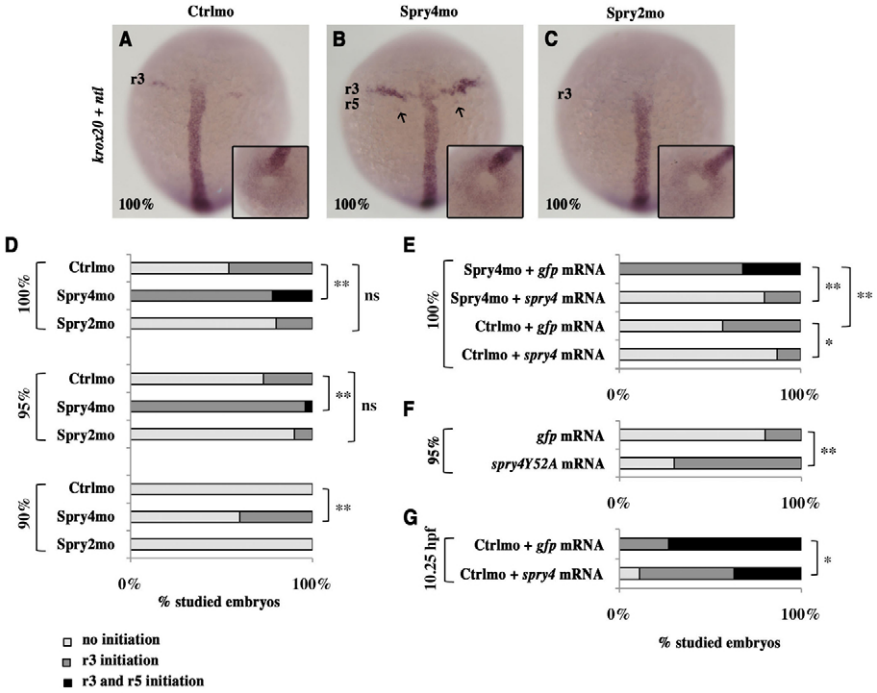

Fig. 3. Spry4 controls the onset of *krox20* expression. (**A-C**) Zebrafish embryos injected with either control morpholino (Ctrlmo) (A), Spry4mo (B) or Spry2mo (C) were collected at 100% epiboly and subjected to in situ hybridisation with *krox20* and *ntl* probes (purple). Arrows in B indicate *krox20* expression in a few r5 cells. The insets show tailbud views of the embryos, allowing determination of the developmental stage by evaluation of the closure of the tailbud, as revealed by *ntl* expression. (**D-G**) Distribution of embryos showing either no *krox20* expression, limited expression in r3 or expression in both r3 and r5 at 90, 95 or 100% epiboly or at 10.25 hours post-fertilisation (hpf). ns, not significant; *, $P<0.05$; **, $P<0.0001$; χ^2-test.

in the hindbrain (see Fig. S6 in the supplementary material), establishing that Spry4 is indeed part of a negative-feedback loop. At 10.25 hpf, only 63% of the SU5402-treated embryos ($n=19$) expressed *krox20* in r3, as compared with 95% of the control embryos ($n=22$; χ^2-test, $P<0.0001$; Fig. 4A,B,E), which in addition showed larger *krox20* expression domains. Furthermore, none of the embryos treated with SU5402 expressed *krox20* in r5, as compared with 50% of the control embryos at this stage. A defect at the level of r5 was still observed at 10.5 hpf (1-somite stage), with no *krox20* expression in SU5402-treated embryos ($n=28$; χ^2-test, $P<0.0001$; Fig. 4C,D,E).

These data were confirmed by an alternative approach. A stable transgenic line that expresses a heat shock-inducible dominant-negative form of Fgfr1 (Lee et al., 2005) was used to downregulate FGF signalling. Expression of the dominant-negative receptor was induced at the 80% epiboly stage and embryos were collected at 10.25 hpf. At this stage, *krox20* was expressed at the level of r3 in 94% of the non-transgenic embryos ($n=72$), in contrast to only 64% of *hsp70l:dnfgfr1-gfp* transgenic embryos ($n=74$; χ^2-test, $P<0.0001$; data not shown). Overall, these results establish that FGF signalling is essential for the normal onset of *krox20* expression in r3 and r5.

FGF signalling controls initiator but not maintenance *krox20* enhancers

Krox20 transcription in r3 and r5 is subject to two regulatory phases controlled by distinct cis-acting regulatory elements (Chomette et al., 2006; Wassef et al., 2008). Transcription is first induced in a cell under the control of initiator enhancers (element C in r3 and elements B and C in r5) leading to the early accumulation of Krox20 protein (the onset phase); this protein can then activate a positive autoregulatory loop by binding to a third enhancer, element A (the amplification and maintenance phase). Our observations of the consequences of the modulation of FGF signalling on early *krox20* expression suggest that this pathway might be required during the onset phase. To test this, we performed the SU5402 treatment on embryos carrying a point mutation in the *krox20* coding sequence that inactivates the protein and therefore prevents the establishment of the autoregulatory loop [$krox20^{fh227/fh227}$ (Monk et al., 2009)]. We found that at the 4-somite stage, the *krox20*-positive territories (corresponding only to the onset phase in the homozygous mutants) were dramatically reduced in SU5402-treated, as compared with DMSO carrier-treated, mutant embryos, as was the case for wild-type embryos (Fig. 4F-I). This definitively demonstrates that FGF signalling affects the onset phase of *krox20* expression.

To investigate whether FGF signalling was acting on *Krox20* at the transcriptional level, we analysed the dependence of the different cis-acting regulatory elements on FGF signalling. We first made use of a chick hindbrain electroporation system that we have shown previously to largely reflect the in vivo activities of the enhancers (Chomette et al., 2006). Constructs in which a GFP reporter is driven by each of the *Krox20* chick enhancers were co-electroporated with expression vectors for wild-type or dominant-negative (Spry4Y52A) HA-tagged forms of Spry4 to modulate FGF signalling. The level of endogenous *Krox20* expression was not affected after electroporation of wild-type ($n=14$; Fig. 5A,B, compare left and right) or Y52A ($n=17$; Fig. 5C,D) Spry4 at the 7- to 8-somite stage [Hamburger-Hamilton (HH) stage 9]. This suggests that endogenous *Krox20* expression is no longer sensitive to FGF signalling at this stage, consistent with previous observations (Aragon and Pujades, 2009). By contrast, co-electroporation with the enhancer constructs revealed that the activities of both the B and C enhancers were significantly reduced when co-electroporated with the wild-type Spry4 construct as compared with the dominant-negative form (59% and 63% reduction, respectively; $n=17$; Fig. 5I-P,R,S). It should be noted that we used a version of element C that contains additional sequences compared with the previously published enhancer (Chomette et al., 2006). This results in a higher specificity of the enhancer for r3 (data not shown). In contrast to its effect on the initiator elements, alteration of FGF signalling had no effect on enhancer A activity (Fig. 5E-H,Q). In conclusion, these data indicate that elements B and C, which are responsible for the onset of *krox20* transcription, are controlled by FGF signalling, whereas element A, which is in charge of the amplification and maintenance phase, is not.

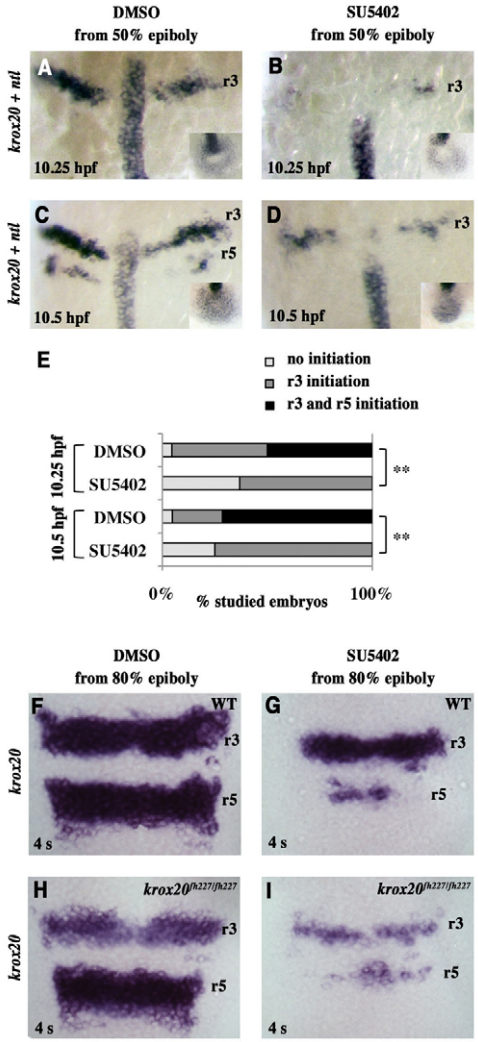

Fig. 4. FGF signalling is required for the appropriate onset of *krox20* expression. (**A-D**,**F-I**) Zebrafish embryos were incubated in either DMSO carrier or SU5402 from 50% epiboly to 10.25 hpf (A,B) or from 50% epiboly to the 1-somite stage (10.5 hpf) (C,D) or from 80% epiboly to the 4-somite stage (F-I) and analysed by in situ hybridisation for *krox20* and *ntl* (A-D) or for *krox20* alone (F-I). The insets in A-D show tailbud views of the corresponding embryos (see Fig. 3). Wild-type (WT) and *krox20*$^{fh227/fh227}$ mutant embryos are compared in F-I. (**E**) Distribution of the embryos according to *krox20* expression in r3 and r5 (see Fig. 3). **, $P<0.0001$; χ^2-test.

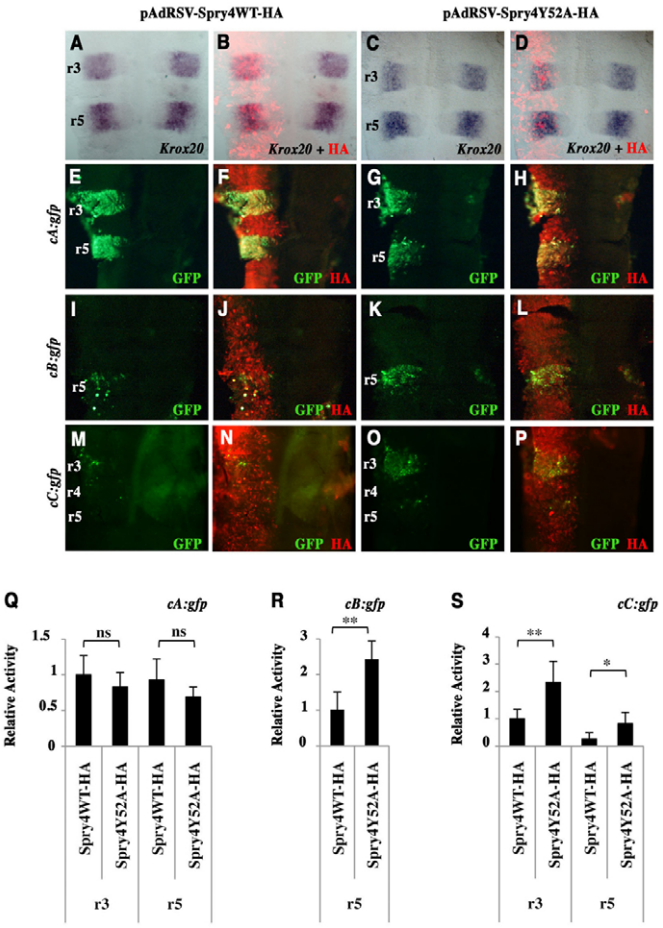

Fig. 5. Spry4 regulates *Krox20* initiator enhancers in the chick embryo. (**A-D**) Chick embryo neural tubes were electroporated on the left side with HA-tagged wild-type or Y52A dominant-negative zebrafish *spry4*-expressing vectors (pAdRSV-Spry4WT-HA and pAdRSV-Spry4Y52A-HA), and flat-mounted after in situ hybridisation with a *Krox20* probe. No difference was detected between the left (experimental) and right (control) sides. The efficiency of electroporation and *spry4* expression were monitored by immunolabelling against the HA tag (B,D). (**E-P**) Chick embryo neural tubes were co-electroporated with HA-tagged wild-type or Y52A dominant-negative *spry4*-expressing vectors and constructs carrying chicken *Krox20* enhancer elements cA, cB or cC driving the *gfp* reporter, and subjected to HA (red) and GFP (green) immunostaining (merge in yellow). (**Q-S**) Quantitative evaluation of relative reporter activity obtained by dividing the GFP signal intensity by the HA signal intensity, both quantified using ImageJ. ns, not significant; *, $P<0.0005$; **, $P<0.0001$; Student's *t*-test. Errors bars indicate s.e.m.

To test whether these finding are also applicable to zebrafish, we generated stable transgenic lines carrying a *gfp* reporter under the control of chick element A (cA; zebrafish element A has not yet been identified) or zebrafish element B (zB). Transgenic embryos were exposed to SU5402 or DMSO carrier from the 1- to 8-somite stages, then fixed and analysed by double in situ hybridisation for *gfp* and *krox20*. In *cA:gfp* transgenic embryos, *gfp* expression always precisely overlapped with *krox20* expression in both r3 and r5, even after SU5402 treatment, which led to a reduction in the size of the r5 territory (n=16 and n=19, respectively; Fig. 6A,B). This suggests that the activity of element A is not affected by FGF signalling (the reduction in the r5 domain of A activity is likely to reflect the consequences of a lack of initiation of *krox20* expression). In *zB:gfp* transgenic embryos, *gfp* expression was restricted to r5 as expected in DMSO-treated control embryos (n=14), and was almost entirely absent from the remaining r5 territory after SU5402 treatment (n=15; Fig. 6C,D), indicating that element B absolutely requires FGF signalling for its activity.

Together, these chick and zebrafish experiments establish that FGF signalling controls *Krox20* transcription by regulating its onset phase through elements B and C. By contrast, the amplification and maintenance phase, controlled by element A, is not dependent on FGFs. This latter point explains why endogenous *Krox20*

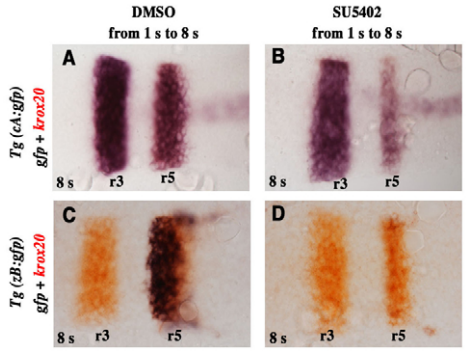

Fig. 6. FGF signalling is required for *krox20* enhancer B activity in the zebrafish embryo. (**A-D**) Transgenic embryos carrying the *gfp* gene under the control of the chicken *Krox20* A enhancer [*Tg(cA:gfp)*] (A,B) or the zebrafish *krox20* B enhancer [*Tg(zB:gfp)*] (C,D) were incubated in DMSO carrier (A,C) or SU5402 (B,D) from the 1-somite stage, collected at the 8-somite stage and subjected to double in situ hybridisation for *gfp* (blue) and *krox20* (orange); overlap is purple (A-C). Embryos were flat-mounted with anterior to the left.

expression is not sensitive (chick) or only partially sensitive (zebrafish) to a block in FGF signalling when the autoregulatory loop has become engaged.

MafB mediates FGF signalling by direct binding to element B

Since the effect of FGF signalling on *Krox20* expression in r5 is at least in part mediated by element B, we searched for the trans-acting factors involved. The transcription factor MafB, which is encoded in zebrafish by *mafba*, is necessary for *Krox20* expression in r5 (Cordes and Barsh, 1994; Moens et al., 1996; Wiellette and Sive, 2003). MafB expression requires FGF signalling (Aragon and Pujades, 2009; Maves et al., 2002; Walshe et al., 2002; Wiellette and Sive, 2003; Wiellette and Sive, 2004). We investigated the dynamics of *mafba* expression and found that Spry4 loss-of-function led to the premature onset of *mafba* in r5/r6: at 95% epiboly, all Spry4 morphants expressed *mafba* (n=28), versus only 12% of control embryos (n=33; χ^2-test, P<0.0001; see Fig. S7 in the supplementary material). These data raise the possibility that the premature onset of *krox20* expression in r5 is due to precocious activation of *mafba*.

To investigate whether MafB directly controls element B, we searched for potential MafB binding sites within enhancer B sequences conserved in vertebrate species. We found two motifs similar to the consensus MafB recognition element (MARE), termed MafB-1 and MafB-2 (Fig. 7A,B). The MafB-1 sequence is conserved between zebrafish, *Xenopus*, chick and mouse (Fig. 7A) and is followed by a sequence of lower similarity to MARE in reverse orientation (Fig. 7A). MafB-2 is well conserved between *Xenopus*, chicken and mouse enhancers, but was not found in the zebrafish enhancer at this position (Fig. 7A), although an identical sequence is present in zebrafish at a more 5′ position. Interestingly, MafB-2 is located close to a vHnf1 (Hnf1ba – Zebrafish Information Network) binding site (Fig. 7A) that we have previously shown to be required for element B activity in r5 (Chomette et al., 2006). We investigated whether MafB interacts with the two putative binding sites by gel retardation. Incubation of oligonucleotides carrying each sequence (Fig. 7A) with bacterially expressed mouse MafB led to the formation of specific retarded bands (Fig. 7C). To establish that the binding sites corresponded to the sequences identified in silico, we introduced mutations into the putative MafB sites (Fig. 7B). Band shift analysis demonstrated that the affinity of MafB was strongly reduced for the mutated MafB-1 oligonucleotide and abolished for the mutated MafB-2 oligonucleotide (Fig. 7C). In the former case, residual binding might be due to the presence of the related sequence in reverse orientation, which was also present in the oligonucleotide.

To investigate the functional significance of these binding sites in the enhancer, we compared the activities of wild-type and mutant versions of chick element B driving the *lacZ* reporter in the chick electroporation system. Wild-type enhancer activity was restricted to r5 as expected (Fig. 7D). Mutation of the MafB-1 or MafB-2 site strongly reduced the activity of element B (Fig. 7E,F) and the double mutation abolished it (Fig. 7G). This demonstrated that both sites are important for enhancer activity. To investigate the ability of MafB to activate the enhancer via these sites and to cooperate with vHnf1, we performed co-electroporation experiments. Co-electroporation of the wild-type enhancer with MafB or vHnf1 expression vectors led to slight expansions of the domain of enhancer activity (Fig. 7H,I). However, co-electroporation with both expression vectors led to generalised and high-level activation of the enhancer throughout the neural tube (Fig. 7J). By contrast, almost all activity was abolished when the enhancer carried mutations in both MafB sites (Fig. 7K) or in the vHnf1 binding site (data not shown). Finally, we analysed endogenous chick *Krox20* expression upon ectopic expression of *MafB*, *vHnf1* or both, and it responded in a manner similar to element B, although the ectopic activation was more limited (see Fig. S8 in the supplementary material).

In conclusion, this analysis establishes that in r5, MafB activates element B and therefore *Krox20* expression by direct binding to the MafB-1 and MafB-2 sites, and that it synergistically cooperates with vHnf1 bound to its nearby cognate site. Since MafB is itself under FGF (Wiellette and Sive, 2003) and Spry4 (this study) control, this demonstrates that in r5, *Krox20* regulation by the FGF pathway and fine-tuning by Spry4 involve direct transcriptional control by MafB.

DISCUSSION

In this study, we have investigated FGF-dependent mechanisms that control the size of rhombomeres during zebrafish hindbrain development. We have established the role of a negative-feedback regulatory loop governed by Spry4, which fine-tunes FGF signalling to control early *krox20* transcription and the subsequent expansion of r3, r4 and r5. The tight correlation between these two processes suggests a direct causative link between them. We propose that fine-tuning, negative-feedback regulation and positive autoregulation can combine at the molecular level to ensure robust and precise patterning.

FGF signalling controls early *krox20* transcription

Previous studies have shown that FGF signalling plays an essential role in the control of *Krox20* expression in r3 and r5 (Aragon and Pujades, 2009; Marin and Charnay, 2000; Maves et al., 2002; Walshe et al., 2002; Wiellette and Sive, 2003; Wiellette and Sive, 2004). Here we investigated the timing, the level of action and the mechanisms of FGF control. We had previously shown that *krox20* is initially transcribed under the control of two initiator cis-acting regulatory elements: C in r3 and r5 and

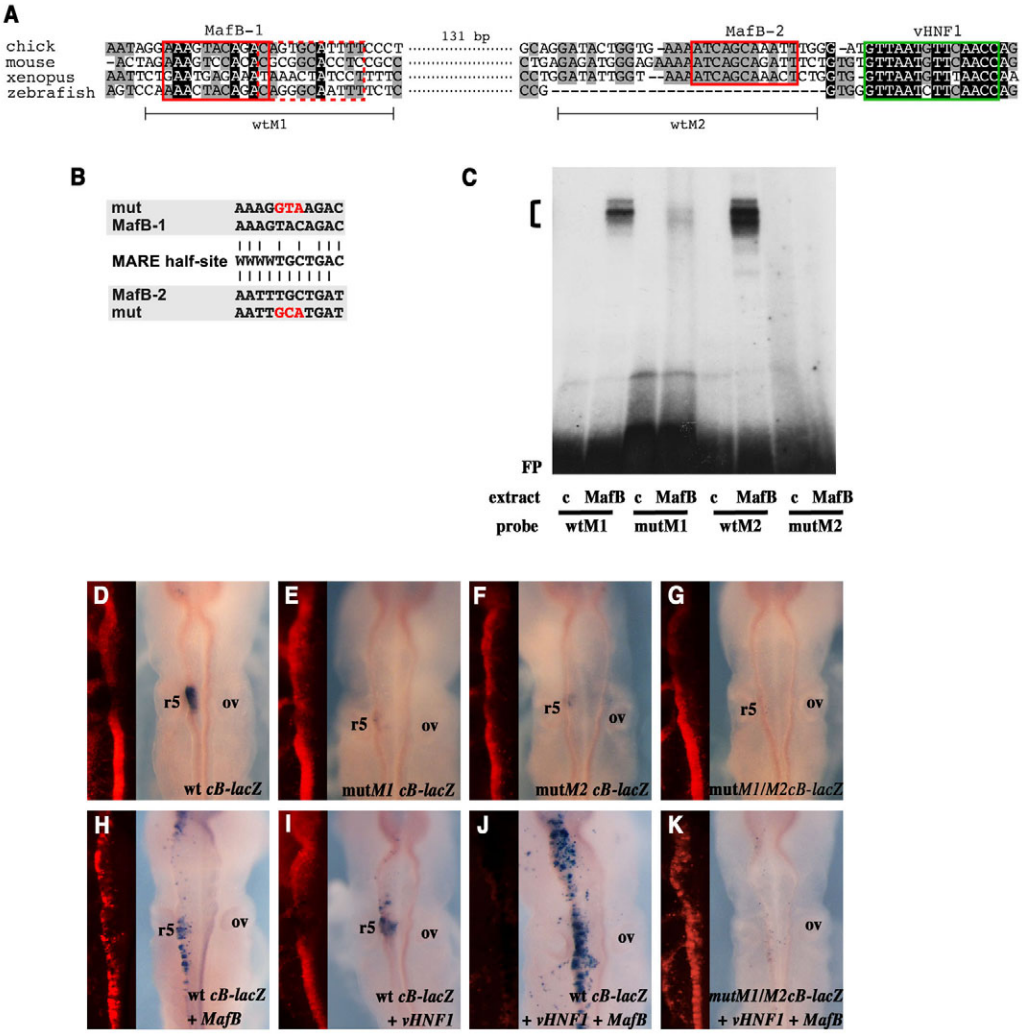

Fig. 7. Identification of functional MafB binding sites in *Krox20* enhancer B. (**A**) Alignment of zebrafish, *Xenopus*, chick and mouse *Krox20* element B nucleotide sequences showing the two conserved putative MafB sites MafB-1 and MafB-2 (red boxes). A sequence of lower similarity to the MafB consensus binding site, adjacent to MafB-1 and in the reverse orientation, is also indicated (dashed red box). A vHnf1 binding site is indicated by the green box. The oligonucleotides used for gel retardation (wtM1 and wtM2) are indicated beneath. (**B**) Alignment of MafB-1 and MafB-2 with the consensus MafB recognition element (MARE) half-site (W=A or T). The mutations introduced into the MafB-1 and MafB-2 sites are indicated in red. (**C**) Gel retardation analyses were performed with the indicated bacterial protein extracts (c, control without MafB protein) and oligonucleotides carrying the chick versions of the MafB-1 and MafB-2 sites, either wild-type (wtM1, wtM2) or mutated (mutM1, mutM2). FP, free probe. The bracket indicates MafB-probe shift complexes, which are abolished or largely abolished by mutation of the MafB-2 and MafB-1 sites, respectively. (**D-K**) Chick embryos were analysed by X-gal staining after electroporation with constructs containing wild-type (D,H-J) or mutant (E-G,K) versions of chick element B driving a β-*globin* promoter-*lacZ* reporter. Embryos were co-electroporated with *MafB* alone (H), *vHnf1* alone (I), or both (J,K). In all cases, a *Cherry*-expressing vector was co-electroporated to monitor electroporation efficiency; Cherry visualisation (red) was carried out following X-gal staining and is shown to the left of each image. Note that strong X-gal staining quenches Cherry fluorescence. ov, otic vesicle.

B in r5 (Chomette et al., 2006; Wassef et al., 2008). Later on, *krox20* expression is amplified and maintained under the control of the autoregulatory enhancer A (Chomette et al., 2006). In this study, using different methods to perturb FGF signalling, we have established that early levels of FGF signalling modulate the onset of *krox20* expression in r3 and r5, i.e. its timing and the expansion of its early domains, whereas *krox20* expression is only marginally dependent on FGF signalling after the 1-somite stage (Fig. 6). Consistently, FGF signalling controls both of the *krox20* initiator enhancers, whereas it has no effect on the autoregulatory element (Figs 5 and 6) and does not require the autoregulatory loop (Fig. 4F-I). Therefore, although we cannot exclude the possibility that FGF signalling also affects *krox20* expression at another level (e.g. translational), all available data converge toward the idea that its major site of action is the onset of transcription.

In the case of r5, we went on to investigate the detailed molecular mechanisms of the pathway. We have shown that the early expression of *krox20* is mediated by direct binding of MafB to enhancer B (Fig. 7). This activation involves vHnf1, which also binds to enhancer B and cooperates synergistically with MafB (Fig. 7). Since the onset of *mafba* expression is itself controlled by FGF signalling (see Fig. S7 in the supplementary material), our data provide a detailed chain of events for the regulation of enhancer B by FGF signalling and ultimately for the control of early *krox20* expression in r5.

Early *krox20* expression sets the blueprint for r3-r5 patterning

The modifications in the onset of *krox20* expression following modulation of FGF signalling correlated with drastic variations in the sizes of mature r3, r4 and r5 at mid-somitogenesis. To explain these correlations, we propose that the number of Krox20-positive cells at early stages actually determines the later size of these territories. This idea is consistent with our current representation of the development of the r3-r5 region. It has been established that the specification of r3 and r5 absolutely requires Krox20 (Schneider-Maunoury et al., 1993; Seitanidou et al., 1997; Swiatek and Gridley, 1993; Voiculescu et al., 2001). As discussed above, *krox20* expression in r3 and r5 is initiated under the control of elements B and C. We propose that once Krox20 levels have reached a certain threshold in a cell, the autoregulatory loop based on element A is switched on. Therefore, the duration of activity of elements B and C required for permanent *krox20* expression in a cell may be very short. In addition, whereas the autoregulatory loop specifies the level of *krox20* expression during the stationary phase, it cannot modulate the number of stably expressing cells, which is determined by the level of *krox20* expression reached under the control of elements B or C and the affinity of the Krox20 binding sites present in element A. Cell proliferation will then contribute to the absolute size of the rhombomeres. However, since the rate of cell proliferation appears to be similar in the different rhombomeres (see Fig. S4 in the supplementary material), it does not affect their relative size.

In conclusion, these results fully support the idea that the mature sizes of r3 and r5 are primarily determined by the number of cells in which *krox20* is initially activated. This link explains why perturbations in FGF signalling, a pathway that precisely modulates the efficiency of initial *krox20* activation, have such dramatic effects on the relative size of the mature rhombomeres. Finally, the development of r4 inversely mirrors the number of cells stably expressing *krox20*, as *krox20* gain-of-function in a cell results in loss of r4 identity, and *krox20* loss-of-function causes a gain of r4 identity (Giudicelli et al., 2001; Voiculescu et al., 2001).

Fine-tuning of early *krox20* expression requires negative-feedback regulation of FGF signalling

As discussed above, we propose that segment formation in the r3-r5 region is based on a bistable cell-fate choice that is dependent on the activation (or not) of the Krox20 positive autoregulatory loop. Such switch-like mechanisms play central roles in the patterning of multicellular organisms (Graham et al., 2010; Kitano, 2004). Here, the binary choice is coupled with the translation of the local FGF concentration into the initial activation of *krox20*. However, because of fluctuations in the environment and in ligand concentration, transcriptional noise and the occurrence of mutations, this type of network organisation is expected to lack precision and robustness (Jaeger et al., 2008). More specifically, if the number of cells that initially activate *krox20* in r3 and r5 is of such importance for hindbrain patterning, a very precise regulation of this aspect of *krox20* expression is likely to be required. A way to buffer fluctuations and to improve precision is to introduce a cell-autonomous negative-feedback loop in the target cells (Freeman, 2000). We think that this is precisely the role of Spry4 in this system. *spry4* is positively regulated by FGF and acts intracellularly to negatively regulate FGF signalling through inhibition of the Ras/MAPK pathway (see Figs S5 and S6 in the supplementary material) (Furthauer et al., 2001; Ozaki et al., 2005; Sasaki et al., 2001). We have shown by loss- and gain-of-function experiments that Spry4 negatively modulates early *krox20* expression (Fig. 3). If a feedback loop is already established when target gene activation occurs, the outcome can be a reduction in fluctuations in expression of the target gene (Brandman and Meyer, 2008). Our system works under these conditions, as the expression of *spry4* precedes that of *krox20* (Fig. 1; data not shown). In addition, release of the antagonistic action of Spry4 is expected to lead to increased expression of the target genes, resulting in premature activation. This is precisely what is observed for *krox20* activation (Fig. 3). In conclusion, the bistable cell-fate choice required for efficient and non-ambiguous hindbrain patterning is likely to impose fine-tuning of FGF control, which is achieved through the establishment of the Spry4 negative-feedback loop.

Acknowledgements

This work was supported by grants to P.C. from INSERM, MESR and ANR. C.L. was supported by FRM and Neuropole Ile-de-France, Y.X.B. by MESR, M.A.W. by MESR and ARC, P.A.G. by the ENS and Fondation Pierre-Gilles de Gennes and J.L.M. by MESR.

Competing interests statement

The authors declare no competing financial interests.

Supplementary material

Supplementary material for this article is available at
http://dev.biologists.org/lookup/suppl/doi:10.1242/dev.057299/-/DC1

References

Aragon, F. and Pujades, C. (2009). FGF signaling controls caudal hindbrain specification through Ras-ERK1/2 pathway. *BMC Dev. Biol.* **9**, 61.
Brandman, O. and Meyer, T. (2008). Feedback loops shape cellular signals in space and time. *Science* **322**, 390-395.
Chomette, D., Frain, M., Cereghini, S., Charnay, P. and Ghislain, J. (2006). Krox20 hindbrain cis-regulatory landscape: interplay between multiple long-range initiation and autoregulatory elements. *Development* **133**, 1253-1262.
Cordes, S. P. and Barsh, G. S. (1994). The mouse segmentation gene kr encodes a novel basic domain-leucine zipper transcription factor. *Cell* **79**, 1025-1034.
Desmazières, A., Charnay, P. and Gilardi-Hebenstreit, P. (2009). Krox20 controls the transcription of its various targets in the developing hindbrain according to multiple modes. *J. Biol. Chem.* **284**, 10831-10840.
Freeman, M. (2000). Feedback control of intercellular signalling in development. *Nature* **408**, 313-319.
Furthauer, M., Thisse, C. and Thisse, B. (1997). A role for FGF-8 in the dorsoventral patterning of the zebrafish gastrula. *Development* **124**, 4253-4264.
Furthauer, M., Reifers, F., Brand, M., Thisse, B. and Thisse, C. (2001). sprouty4 acts in vivo as a feedback-induced antagonist of FGF signaling in zebrafish. *Development* **128**, 2175-2186.
Furthauer, M., Lin, W., Ang, S. L., Thisse, B. and Thisse, C. (2002). Sef is a feedback-induced antagonist of Ras/MAPK-mediated FGF signalling. *Nat. Cell Biol.* **4**, 170-174.
Furthauer, M., Van Celst, J., Thisse, C. and Thisse, B. (2004). Fgf signalling controls the dorsoventral patterning of the zebrafish embryo. *Development* **131**, 2853-2864.
Ghislain, J., Desmarquet-Trin-Dinh, C., Gilardi-Hebenstreit, P., Charnay, P. and Frain, M. (2003). Neural crest patterning: autoregulatory and crest-specific elements co-operate for Krox20 transcriptional control. *Development* **130**, 941-953.
Giudicelli, F., Taillebourg, E., Charnay, P. and Gilardi-Hebenstreit, P. (2001). Krox-20 patterns the hindbrain through both cell-autonomous and non cell-autonomous mechanisms. *Genes Dev.* **15**, 567-580.
Graham, T. G., Tabei, S. M., Dinner, A. R. and Rebay, I. (2010). Modeling bistable cell-fate choices in the Drosophila eye: qualitative and quantitative perspectives. *Development* **137**, 2265-2278.
Gross, I., Bassit, B., Benezra, M. and Licht, J. D. (2001). Mammalian sprouty proteins inhibit cell growth and differentiation by preventing ras activation. *J. Biol. Chem.* **276**, 46460-46468.
Hacohen, N., Kramer, S., Sutherland, D., Hiromi, Y. and Krasnow, M. A. (1998). sprouty encodes a novel antagonist of FGF signaling that patterns apical branching of the Drosophila airways. *Cell* **92**, 253-263.
Hauptmann, G. and Gerster, T. (1994). Two-color whole-mount in situ hybridization to vertebrate and Drosophila embryos. *Trends Genet.* **10**, 266.
Jaeger, J., Irons, D. and Monk, N. (2008). Regulative feedback in pattern formation: towards a general relativistic theory of positional information. *Development* **135**, 3175-3183.

Kitano, H. (2004). Biological robustness. *Nat. Rev. Genet.* **5**, 826-837.
Komisarczuk, A. Z., Topp, S., Stigloher, C., Kapsimali, M., Bally-Cuif, L. and Becker, T. S. (2008). Enhancer detection and developmental expression of zebrafish sprouty1, a member of the fgf8 synexpression group. *Dev. Dyn.* **237**, 2594-2603.
Lee, Y., Grill, S., Sanchez, A., Murphy-Ryan, M. and Poss, K. D. (2005). Fgf signaling instructs position-dependent growth rate during zebrafish fin regeneration. *Development* **132**, 5173-5183.
Lumsden, A. (1990). The cellular basis of segmentation in the developing hindbrain. *Trends Neurosci.* **13**, 329-335.
Lumsden, A. and Keynes, R. (1989). Segmental patterns of neuronal development in the chick hindbrain. *Nature* **337**, 424-428.
Lumsden, A. and Krumlauf, R. (1996). Patterning the vertebrate neuraxis. *Science* **274**, 1109-1115.
Manzanares, M., Nardelli, J., Gilardi-Hebenstreit, P., Marshall, H., Giudicelli, F., Martinez-Pastor, M. T., Krumlauf, R. and Charnay, P. (2002). Krox20 and kreisler co-operate in the transcriptional control of segmental expression of Hoxb3 in the developing hindbrain. *EMBO J.* **21**, 365-376.
Marin, F. and Charnay, P. (2000). Hindbrain patterning: FGFs regulate Krox20 and mafB/kr expression in the otic/preotic region. *Development* **127**, 4925-4935.
Maves, L., Jackman, W. and Kimmel, C. B. (2002). FGF3 and FGF8 mediate a rhombomere 4 signaling activity in the zebrafish hindbrain. *Development* **129**, 3825-3837.
Minowada, G., Jarvis, L. A., Chi, C. L., Neubuser, A., Sun, X., Hacohen, N., Krasnow, M. A. and Martin, G. R. (1999). Vertebrate Sprouty genes are induced by FGF signaling and can cause chondrodysplasia when overexpressed. *Development* **126**, 4465-4475.
Moens, C. B., Yan, Y. L., Appel, B., Force, A. G. and Kimmel, C. B. (1996). valentino: a zebrafish gene required for normal hindbrain segmentation. *Development* **122**, 3981-3990.
Moens, C. B., Cordes, S. P., Giorgianni, M. W., Barsh, G. S. and Kimmel, C. B. (1998). Equivalence in the genetic control of hindbrain segmentation in fish and mouse. *Development* **125**, 381-391.
Monk, K. R., Naylor, S. G., Glenn, T. D., Mercurio, S., Perlin, J. R., Dominguez, C., Moens, C. B. and Talbot, W. S. (2009). A G protein-coupled receptor is essential for Schwann cells to initiate myelination. *Science* **325**, 1402-1405.
Muller, M. V., Weizsacker, E. and Campos-Ortega, J. A. (1996). Expression domains of a zebrafish homologue of the Drosophila pair-rule gene hairy correspond to primordia of alternating somites. *Development* **122**, 2071-2078.
Oxtoby, E. and Jowett, T. (1993). Cloning of the zebrafish krox-20 gene (krx-20) and its expression during hindbrain development. *Nucleic Acids Res.* **21**, 1087-1095.
Ozaki, K., Miyazaki, S., Tanimura, S. and Kohno, M. (2005). Efficient suppression of FGF-2-induced ERK activation by the cooperative interaction among mammalian Sprouty isoforms. *J. Cell Sci.* **118**, 5861-5871.
Pezeron, G., Lambert, G., Dickmeis, T., Strahle, U., Rosa, F. M. and Mourrain, P. (2008). Rasl11b knock down in zebrafish suppresses one-eyed-pinhead mutant phenotype. *PLoS ONE* **3**, e1434.
Prince, V. E., Moens, C. B., Kimmel, C. B. and Ho, R. K. (1998). Zebrafish hox genes: expression in the hindbrain region of wild-type and mutants of the segmentation gene, valentino. *Development* **125**, 393-406.
Robu, M. E., Larson, J. D., Nasevicius, A., Beiraghi, S., Brenner, C., Farber, S. A. and Ekker, S. C. (2007). p53 activation by knockdown technologies. *PLoS Genet.* **3**, e78.
Roy, N. M. and Sagerstrom, C. G. (2004). An early Fgf signal required for gene expression in the zebrafish hindbrain primordium. *Brain Res. Dev. Brain Res.* **148**, 27-42.
Sasaki, A., Taketomi, T., Wakioka, T., Kato, R. and Yoshimura, A. (2001). Identification of a dominant negative mutant of Sprouty that potentiates fibroblast growth factor- but not epidermal growth factor-induced ERK activation. *J. Biol. Chem.* **276**, 36804-36808.
Schneider-Maunoury, S., Topilko, P., Seitandou, T., Levi, G., Cohen-Tannoudji, M., Pournin, S., Babinet, C. and Charnay, P. (1993). Disruption of Krox-20 results in alteration of rhombomeres 3 and 5 in the developing hindbrain. *Cell* **75**, 1199-1214.
Schneider-Maunoury, S., Seitanidou, T., Charnay, P. and Lumsden, A. (1997). Segmental and neuronal architecture of the hindbrain of Krox-20 mouse mutants. *Development* **124**, 1215-1226.
Schulte-Merker, S., Hammerschmidt, M., Beuchle, D., Cho, K. W., De Robertis, E. M. and Nusslein-Volhard, C. (1994). Expression of zebrafish goosecoid and no tail gene products in wild-type and mutant no tail embryos. *Development* **120**, 843-852.
Seitanidou, T., Schneider-Maunoury, S., Desmarquet, C., Wilkinson, D. G. and Charnay, P. (1997). Krox-20 is a key regulator of rhombomere-specific gene expression in the developing hindbrain. *Mech. Dev.* **65**, 31-42.
Stedman, A., Lecaudey, V., Havis, E., Anselme, I., Wassef, M., Gilardi-Hebenstreit, P. and Schneider-Maunoury, S. (2009). A functional interaction between Irx and Meis patterns the anterior hindbrain and activates krox20 expression in rhombomere 3. *Dev. Biol.* **327**, 566-577.
Swiatek, P. J. and Gridley, T. (1993). Perinatal lethality and defects in hindbrain development in mice homozygous for a targeted mutation of the zinc finger gene Krox20. *Genes Dev.* **7**, 2071-2084.
Voiculescu, O., Taillebourg, E., Pujades, C., Kress, C., Buart, S., Charnay, P. and Schneider-Maunoury, S. (2001). Hindbrain patterning: Krox20 couples segmentation and specification of regional identity. *Development* **128**, 4967-4978.
Walshe, J., Maroon, H., McGonnell, I. M., Dickson, C. and Mason, I. (2002). Establishment of hindbrain segmental identity requires signaling by FGF3 and FGF8. *Curr. Biol.* **12**, 1117-1123.
Wassef, M. A., Chomette, D., Pouilhe, M., Stedman, A., Havis, E., Desmarquet-Trin Dinh, C., Schneider-Maunoury, S., Gilardi-Hebenstreit, P., Charnay, P. and Ghislain, J. (2008). Rostral hindbrain patterning involves the direct activation of a Krox20 transcriptional enhancer by Hox/Pbx and Meis factors. *Development* **135**, 3369-3378.
Wiellette, E. L. and Sive, H. (2003). vhnf1 and Fgf signals synergize to specify rhombomere identity in the zebrafish hindbrain. *Development* **130**, 3821-3829.
Wiellette, E. L. and Sive, H. (2004). Early requirement for fgf8 function during hindbrain pattern formation in zebrafish. *Dev. Dyn.* **229**, 393-399.
Wilkinson, D. G., Bhatt, S., Chavrier, P., Bravo, R. and Charnay, P. (1989). Segment-specific expression of a zinc-finger gene in the developing nervous system of the mouse. *Nature* **337**, 461-464.
Yee, S. P. and Rigby, P. W. (1993). The regulation of myogenin gene expression during the embryonic development of the mouse. *Genes Dev.* **7**, 1277-1289.
Yusoff, P., Lao, D. H., Ong, S. H., Wong, E. S., Lim, J., Lo, T. L., Leong, H. F., Fong, C. W. and Guy, G. R. (2002). Sprouty2 inhibits the Ras/MAP kinase pathway by inhibiting the activation of Raf. *J. Biol. Chem.* **277**, 3195-3201.